2598 *Chem. Mater.* **2009,** *21,* 2598–2600
DOI:10.1021/cm9009282

CHEMISTRY OF MATERIALS
Communication

A Simple and Effective Way of Achieving Highly Efficient and Thermally Stable Bulk-Heterojunction Polymer Solar Cells Using Amorphous Fullerene Derivatives as Electron Acceptor

Yong Zhang,[†] Hin-Lap Yip,[†,‡] Orb Acton,[†] Steven K. Hau,[†] Fei Huang,[†,‡] and Alex K.-Y. Jen*[,†,‡]

[†]*Department of Materials Science and Engineering and* [‡]*Institute of Advanced Materials and Technology, University of Washington, Seattle, Washington 98195*

Received April 2, 2009
Revised Manuscript Received May 11, 2009

Polymer solar cells have been considered as a promising alternative for renewable energy because of their potential for low-cost manufacturing.[1] Until now, the most efficient solar cell was based on the bulk-heterojunction (BHJ) devices composed of a blend of poly(3-hexylthiophene) (P3HT) electron donor and [6,6]-phenyl C_{61} butyric acid methyl ester ($PC_{61}BM$) electron acceptor that showed a power conversion efficiency (PCE) of ~5%.[2] Within the BHJ film, it is critical to control the morphology of the blend to form an interpenetrating network with nanoscale phase separation between the donor and the acceptor at a distance of ~10 nm to maximize exciton dissociation and provide an effective pathway for charge transport and collection.[3] The optimum morphology can be achieved by controlling the kinetics of segregation and crystallization of the components through careful adjustment of the parameters involved in the fabrication processes, such as solvent, blend ratio, thermal annealing, and other post treatment conditions.[2] However, such a phase-separated morphological structure is not very thermodynamically stable because small molecules like PCBM and even polymers like P3HT can still have certain freedom to diffuse slowly or recrystallize over time especially under elevated temperatures.[4] This gradual change in the microstructure will lead to reduced number of interfaces and result in degrading the performance of the device. This is detrimental to the long-term performance of polymer solar cells.[5]

Recently, several strategies have been developed to improve thermal and morphological stability of the polymer:fullerene BHJ cells. For example, by modifying polythiophenes with controlled amount of disorder in their backbone, it can suppress the crystallization-driven phase separation between the polymer and fullerene during thermal annealing.[6] By introducing diblock copolymer additives in the BHJ film, it can also stabilize the device structure against destructive thermal phase segregation.[7] Using a BHJ film in which both polymer and fullerene are substituted with similar chemical motif is also an effective way to stabilize the nanophase segregation between the donor−acceptor pair.[8]

Herein, we report a simple and effective approach to improve thermal stability of BHJ solar cells through the introduction of new amorphous fullerene derivatives as electron-accepting materials. The newly synthesized fullerenes are based on the modifications of PCBM by replacing the planar phenylene ring with a bulky triphenylamine (TPA) or 9,9-dimethylfluorene (MF) aimed at surpressing the crystallization of the resulting compunds. In addition, the electron-donating properties of TPA and MF can increase the LUMO level of the parent fullerene, which is beneficial for achieving higher open circuit voltage (V_{oc}) in BHJ cells.[9] The synthesis, electrochemical, thermal, and electrical properties of the new PCBM derivatives and the performance and thermal stability of the resulting P3HT:new PCBMs BHJ solar cells will be discussed.

The synthetic route for modified fullerenes is shown in Scheme 1. Compounds **1** and **3** were synthesized by Friedel−Crafts acylation between triphenylamine and 9,9-dimethylfluorene using anhydrous $AlCl_3$ as catalyst. They were then reacted with *p*-tosylhydrazide in methanol under refluxing condition to give compounds **2** and **4**, respectively. Followed by treating with sodium methoxide in dried pyridine, it afforded diazo compounds, which were used directly to react with C_{60} in dried *o*-dichlorobenzene

*Corresponding author.

(1) (a) Brabec, C. J.; Sariciftci, N. S.; Hummelen, C. J. *Adv. Funct. Mater.* **2001**, *11*, 15. (b) Krebs, F. C.; Jørgensen, M.; Norrman, K.; Hagemann, O.; Alstrup, J.; Nielsen, T. D.; Fyenbo, J.; Larsen, K.; Kristensen, J. *Sol. Energy Mater. Sol. Cells* **2009**, *93*, 422. (c) Krebs, F. C. *Sol. Energy Mater. Sol. Cells* **2009**, *93*, 394.
(2) (a) Li, G.; Shrotriya, V.; Huang, J.; Yao, Y.; Moriarty, T.; Emery, K.; Yang, Y. *Nat. Mater.* **2005**, *4*, 864. (b) Peet, J.; Kim, J. Y.; Coates, N. E.; Ma, W. L.; Moses, D.; Heeger, A. J.; Bazan, G. C. *Nat. Mater.* **2007**, *6*, 497. (c) Ma, W. L.; Yang, C. Y.; Gong, X.; Lee, K.; Heeger, A. J. *Adv. Funct. Mater.* **2005**, *15*, 1617. (d) Yip, H.-L.; Hau, S. K.; Baek, N. S.; Ma, H.; Jen, A. K.-Y. *Adv. Mater.* **2008**, *20*, 2376. (e) Yip, H. L.; Hau, S. K.; Beak, N. S.; Jen, A. K.-Y. *Appl. Phys. Lett.* **2008**, *92*, 193313. (f) Irwin, M. D.; Buchholz, D. B.; Hains, A. W.; Chang, R. P. H.; Marks, T. J. *Proc. Natl. Acad. Sci. U.S.A.* **2008**, *105*, 2783.
(3) (a) Hoppe, H.; Sariciftci, N. S. *J. Mater. Chem.* **2006**, *16*, 45. (b) Kim, Y. K.; Cook, S.; Choulis, S. A.; Nelson, J.; Durrant, J. R.; Bradley, D. D. C. *Chem. Mater.* **2004**, *16*, 4812.
(4) (a) Swinnen, A.; Haeldermans, I.; vande Ven, M.; D'Haen, J.; Vanhoyland, G.; Aresu, S.; D'Olieslaeger, M. D.; Manca, J. *Adv. Funct. Mater.* **2005**, *16*, 760. (b) Muller, C.; Ferenczi, T. A. M.; Campoy-Quiles, M.; Frost, J. M.; Bradley, D. D. C.; Smith, P.; Stingelin-Stutzmann, N.; Nelson, J. *Adv. Mater.* **2008**, *20*, 3510.
(5) Jørgensen, M.; Norrman, K.; Krebs, F. C. *Sol. Energy Mater. Sol. Cells* **2008**, *92*, 686.
(6) (a) Woo, C. H.; Thompson, B. C.; Kim, B. J.; Toney, M. F.; Fréchet, J. M. J. *J. Am. Chem. Soc.* **2008**, *130*, 16324. (b) Sivula, K.; Luscombe, C. K.; Thompson, B. C.; Fréchet, J. M. J. *J. Am. Chem. Soc.* **2006**, *128*, 13988.
(7) Sivula, K.; Ball, Z. T.; Watanabe, N.; Fréchet, J. M. J. *Adv. Mater.* **2006**, *18*, 206.
(8) Zhou, Z. Y.; Chen, X. W.; Holdcroft, S. *J. Am. Chem. Soc.* **2008**, *130*, 11711.
(9) Kooistra, F. B.; Knol, J.; Kastenberg, F.; Popescu, M.; Verhees, W. J. H.; Kroon, J. M.; Hummelen, J. C. *Org. Lett.* **2007**, *9*, 551.

 Published on Web 06/08/2009

Scheme 1. Synthetic Scheme of TPA-PCBM and MF-PCBM

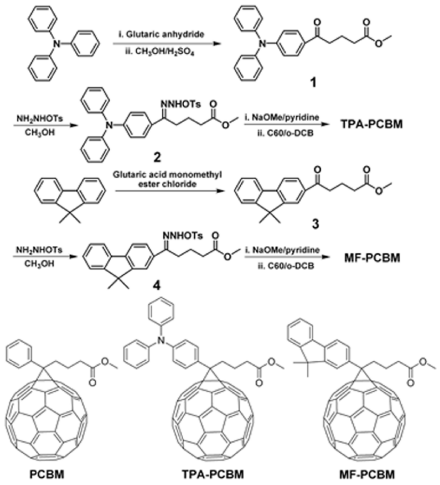

without any purification using the reported methods.[10] The resulting PCBMs were purified through silica column with toluene as eluent to give TPA-PCBM and MF-PCBM with 30−40% yields. As previously reported, the [5,6]-open and [6,6]-closed isomers of [60]methanofullerene could coexist in the cycloaddition reaction of diazo and [60]fullerene. Therefore, it is necessary to treat these isomers in refluxing *o*-dichlorobenzene or toluene to form the more stable [6,6]-closed [60]methanofullerene.[10] The resulting [6,6]-closed [60]methanofullerenes could be easily dissolved in common organic solvents, such as chloroform, toluene, chlorobenzene, and *o*-dichlorobenzene.

The electrochemical properties of TPA-PCBM and MF-PCBM were studied by cyclic voltammetry in 1,2-dichlorobenzene solution with $TBAPF_6$ as electrolyte. As shown in Figure S1 of the Supporting Information, all fullerenes possess four quasireversible one-electron reduction waves, which are attributed to the fullerene core. The first reduction potential (E_1^{red}) corresponding to the LUMO level of PCBM is shifted to more negative value compared to parent C_{60} (shown in Figure S1 of the Supporting Information) because of the decrease in the π-electrons and the release of strain energy after introducing [6,6] methene substitute in C_{60}.[10] Moreover, the reduction waves of TPA-PCBM and MF-PCBM shifted toward more negative potentials compared to that of PCBM as a result of the stronger electron-donating properties of triphenylamine and 9,9-dimethylfluorene compared to that of benzene.

Differential scanning calorimetry (DSC) trace curves of PCBM, TPA-PCBM and MF-PCBM are shown in Figure 1. PCBM shows a crystallization peak at 295 °C with no other transition found between 20 and 350 °C. However, there are no crystallization transitions found in the curves of TPA-PCBM and MF-PCBM, instead, two glass transitions (T_g) were detected at 170 and 180 °C for TPA-PCBM and MF-PCBM, respectively. From the DSC results, it indicates that both TPA-PCBM and MF-PCBM are amphorous materials.

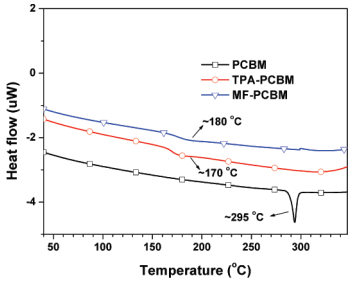

Figure 1. DSC curves of PCBM, TPA-PCBM, and MF-PCBM.

The electron mobility of n-type acceptor is one of the most important factors for high-performance BHJ polymer solar cells. To compare the electron-transporting properties between PCBM and TPA-/MF-PCBMs, n-channel organic field-effect transistors (OFETs) were fabricated. All PCBMs showed typical n-type OFET behavior and the measured saturation field-effect electron mobilities of PCBM, TPA-PCBM and MF-PCBM are 1.6×10^{-2}, 1.1×10^{-2}, and 5.4×10^{-3} cm^2 V^{-1} s^{-1}, respectively (shown in Figure S2). The slight reduction in electron mobilities of TPA-PCBM and MF-PCBM compared to PCBM are attributed to the relatively bulky size of triphenylamine and dimethylfluorene.

The performance of the P3HT:PCBMs BHJ devices were investigated using an inverted cell structure (ITO/ZnO/C_{60}-SAM/P3HT:PCBMs/PEDOT:PSS/Ag) fabricated according to the literature-reported procedure.[11] This inverted structure using more stable and solution-processed metal as the top electrode can provide better ambient stability and cost advantage than the conventional structure.[11c,11d,12] The optimized device performance for each P3HT/PCBMs system was achieved at a blending ratio of 1:0.7 by weight with 10−30 min annealing at 150 °C. The details of the device fabrication and characterization are discussed in the Supporting Information. Figure 2a shows the $J-V$ characteristics of P3HT/PCBMs devices under AM 1.5 G illumination with an intensity of 100 mW cm^{-2}. The power conversion efficiency for TPA-PCBM and MF-PCBM is 4.0% and 3.8%, respectively, which is comparable to that derived from PCBM (4.2%). The TPA-PCBM and MF-PCBM devices had a V_{oc} of 0.65 V, whereas the PCBM device had a V_{oc} of 0.63 V. A 20 mV increase in V_{oc} was observed, which is in agreement with the shift of the LUMO levels as observed in cyclic voltammetry. The current densities (J_{sc}) of TPA-PCBM and MF-PCBM-based devices are 9.9 and 9.8 mA cm^{-2}, respectively, which are slightly lower than that of PCBM device (10.4 mA cm^{-2}) because of lower electron mobilities of the new PCBMs. These

(10) (a) Hummelen, J. C.; Knight, B. W.; Peq, F. L.; Wudl, F. *J. Org. Chem.* **1995**, *60*, 532. (b) Zheng, L. P.; Zhou, Q. M.; Deng, X. Y.; Yuan, M.; Yu, G.; Cao, Y. *J. Phys. Chem. B* **2004**, *108*, 11921. (c) Yang, C.; Kim, J. Y.; Cho, S.; Lee, J. K.; Heeger, A. J.; Wudl, F. *J. Am. Chem. Soc.* **2008**, *130*, 6444.

(11) (a) Hau, S. K.; Yip, H.-L.; Ma, H.; Jen, A. K.-Y. *Appl. Phys. Lett.* **2008**, *93*, 233304. (b) Hau, S. K.; Yip, H. L.; Baek, N. S.; Ma, H.; Jen, A. K.-Y. *J. Mater. Chem.* **2008**, *18*, 5113. (c) Hau, S. K.; Yip, H.-L.; Baek, N. S.; Zou, J.; O'Malley, K.; Jen, A. K.-Y. *Appl. Phys. Lett.* **2008**, *92*, 253301. (d) Hau, S. K.; Yip, H.-L.; Leong, K.; Jen, A. K.-Y. *Org. Electron.* **2009**, *10*, 719.

(12) (a) Krebs, F. C. *Sol. Energy Mater. Sol. Cells* **2008**, *92*, 715. (b) Krebs, F. C. *Sol. Energy Mater. Sol. Cells* **2009**, *93*, 465. (c) Krebs, F. C.; Thomann, Y.; Thomann, R.; Andreasen, J. W. *Nanotechnology* **2008**, *19*, 424013.

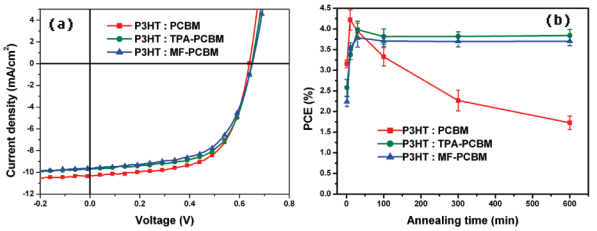

Figure 2. (a) The $J-V$ curves of PCBM-, TPA-PCBM-, and MF-PCBM-based BHJ devices under AM1.5 illumination at 100 mW/cm^2. (b) Plot of PCE vs annealing time of PCBM-, TPA-PCBM-, and MF-PCBM-based devices annealed at 150 °C.

results show that TPA-PCBM and MF-PCBM are very promising electron acceptors that give comparable performance to PCBM-derived devices under similar fabrication conditions.

Thermal stability of the photovoltaic devices using these acceptors were examined by annealing the BHJ films at 150 °C for a time period from 10 min to 10 h. This is a typical temperature for the post-treatment of P3HT:PCBM system.[2c] Figure 2b shows the dependence of PCE on the annealing time of different systems. The highest PCE for the P3HT:PCBM BHJ cell was obtained from the device that was annealed for 10 min. Prolonged annealing results in gradual degradation in device performance with the PCE dropping from 4.2 to 1.8% after annealing for 10 h (Figure 2b). The short circuit current and fill factor also show a gradual decrease with the increase of annealing time (see Figure S3a in the Supporting Information). Thermal stability of both TPA-PCBM and MF-PCBM based devices is significantly better than that of PCBM-based device. Even after extended time of annealing (10 h), there is no obvious loss in device performance (PCE, J_{sc}, and FF), with PCE remaining at ~4% for both types of devices.

To understand the origin of the improved thermal stability in the amorphous PCBMs-based devices, we studied the effect of thermal annealing on phase segregation in the BHJ films. Figure 3 shows the optical micrograph of different BHJ films after being annealed at 150 °C for 10 h. In the case of P3HT:PCBM films, PCBM aggregated and formed microcrystallites that became larger with longer annealing time. This results in a crystal with size up to hundreds of micrometers in length, tens of micrometers in width, and several hundred nanometers in height as revealed by both optical microscopy and atomic force microscopy (AFM) (see Figures S4 and S5 in the Supporting Information). As reported earlier,[6,7] the micrometer-size crystallization of PCBM causes the reduction of interfacial density between the donor and the acceptor, resulting in decreased excition dissociation efficiency and magnitude of photocurrent. On the contrary, both TPA-PCBM- and MF-PCBM-based BHJ films show no sign of destructive phase segregation even after being annealed for 10 h. A homogeneous and smooth surface topology was observed by AFM for both blend films with the surface rms roughness in the range of 1.3−1.5 nm. (Figure S5b and c in the Supporting Information).

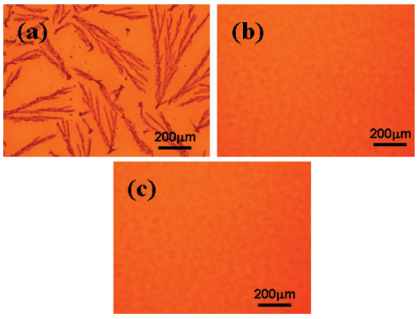

Figure 3. Optical images of (a) P3HT:PCBM, (b) P3HT:TPA-PCBM, and (c) P3HT: MF-PCBM films after annealing at 150 °C for 600 min.

Furthermore, the absorption spectra of the blend films annealed at different time lengths (0, 30, and 600 min) were also studied (see Figure S6 in the Supporting Information). After being annealed for 30 min, three vibronic peaks from the absorption of P3HT (510, 550, and 600 nm) became more pronounced for all the blend films, indicating a higher degree of $\pi-\pi$ stacking of P3HT chains. Further annealing of TPA-PCBM- and MF-PCBM-based films to 600 min did not result in any further change in shape and intensity of the absorption spectrum, which can be correlated to the enhanced thermal stability of devices. However, the P3HT:PCBM film showed a dramatic decrease in PCBM absorption peak at 335 nm because of the severe segregation of PCBM and a further increase in P3HT vibronic peaks that may be due to improved packing in the P3HT-rich phase.

In conclusion, we have reported the synthesis and application of triphenylamine and dimethylfluorene-substituted PCBMs as new acceptor materials for BHJ polymer solar cells. These new compounds show comparable electron mobility to PCBM in OFETs and high power conversion efficiency (~4%) in polymer solar cells. More significantly, thermal stability of the polymer solar cells are remarkably enhanced by suppressing the destructive phase segregation between the polymer and fullerene due to the amorphous nature and high glass-transition temperature of the new PCBMs. For these new amorphous PCBMs, we found no significant degradation in morphology or solar cell performance even after 10 h annealing at 150 °C, whereas a device based on conventional PCBM degraded dramatically against long-time annealing. These results suggest that these new acceptors are very attractive candidates for improving the long-term stability of BHJ polymer solar cells.

Acknowledgment. The authors acknowledge the support of the National Science Foundation's STC program under DMR-0120967 and the DOE "Future Generation Photovoltaic Devices and Process" program under Project DE-FC36-08GO18024/A000. A.K.Y.J. thanks the Boeing-Johnson Foundation for the financial support.

Supporting Information Available: Detailed information about synthesis, characterization, and device fabrication conditions (PDF). This material is available free of charge via the Internet at http://pubs.acs.org.